# Activation of $O_2$ on a Photochemically Generated $Rh^I$ Site on an $Al_2O_3$ Surface: Low-Temperature $O_2$ Dissociation and CO Oxidation

**Edward A. Wovchko and John T. Yates, Jr.***

*Contribution from the Surface Science Center, Department of Chemistry, University of Pittsburgh, Pittsburgh, Pennsylvania 15260*

*Received April 13, 1998*

**Abstract:** The ultraviolet (3.8-eV) photolysis of atomically dispersed $Rh^I(CO)_2$ species supported on an $Al_2O_3$ surface in the presence of $O_2$ at 174 K has been studied by transmission infrared spectroscopy (FTIR). Dioxygen is activated on photochemically generated $Rh^I(CO)$ sites to produce oxidized rhodium carbonyl species and carbon dioxide. A new infrared band in the C−O stretching region is observed at 2156 $cm^{-1}$ and assigned to $Rh^{IV}(CO)(O)_2$ species. A second C−O infrared band is observed at 2122 $cm^{-1}$ and is assigned to $Rh^{II}(CO)O$ species. The $Rh^{IV}(CO)(O)_2$ species is a precursor to $CO_2$ formation. An infrared band at 2344 $cm^{-1}$ is produced by photochemically generated $CO_2$ species which are then adsorbed on the $Al_2O_3$ support. Infrared band assignments are supported by a photochemical $O_2$ activation experiment using doubly isotopically labeled $Rh^I(^{13}C^{18}O)_2$ species. This work demonstrates a low-temperature route for the oxidation of CO on catalyst sites using ultraviolet light as an energy source.

## 1. Introduction

The ultraviolet photolysis of $Rh^I(CO)_2$ supported on an $Al_2O_3$ surface (designated $Rh^I(CO)_2/Al_2O_3$) results in the production of surface sites capable of activating chemical bonds, such as the C−H bond in alkanes and the C═O bond in $CO_2$. This interesting bond activation process demonstrates the first step in a route for the utilization of molecules such methane and $CO_2$ to produce other useful products, heterogeneously. By photolyzing the $Rh^I(CO)_2$ species with 325-nm (3.8-eV) ultraviolet light at low temperatures (<300 K), a CO ligand is easily detached to produce a monocarbonyl species, $Rh^I(CO)$. We have found that this coordinatively unsaturated $Rh^I$ center adsorbs dinitrogen,[1] breaks the C−H bond in alkanes,[2−5] breaks the H−H bond in hydrogen,[6] and breaks the C═O bond in $CO_2$.[7] In this study, we have successfully activated the O═O bond of oxygen using the photochemical production of $Rh^I(CO)/Al_2O_3$ sites.

In the early work of Yang and Garland,[8] the thermally driven oxidation of CO chemisorbed on supported Rh samples was investigated. They discovered that the oxidation of $Rh^I(CO)_2$ species takes place at elevated temperatures (∼443 K) to form carbon dioxide, and they detected the formation of an oxygenated-rhodium carbonyl species which displayed a high-frequency carbonyl infrared band which they assigned to Rh(CO)(O) species. A much more extensive infrared study was later conducted by Rice et al.[9] on the $CO/Rh/Al_2O_3$ system. The oxidation state of the Rh was deduced by preparing rhodium carbonyl species that exhibited distinctive features in their carbonyl infrared spectrum. Higher infrared carbonyl frequencies indicated a higher Rh oxidation state. This work and an additional study by Wey et al.[10] confirmed the formation of Rh(CO)(O) species during elevated-temperature and high-pressure (100−9000-Torr) oxygen exposures. A rhodium oxidation state of II was proposed for this species.[9,10]

By employing infrared spectroscopy, ultrahigh-vacuum techniques, and ultraviolet light, we have been able to observe and control the extent of CO oxidation on atomically dispersed $Rh^I$ sites on $Al_2O_3$ at low temperatures (174 K). In the presence of $O_2$, intermediate rhodium carbonyl species produced prior to CO oxidation are observed. A new $Rh^{IV}(CO)(O)_2$ species has been identified. Carbon dioxide is ultimately produced. A mechanism for the photoassisted oxidation of CO on $Rh^I(CO)$ sites is proposed.

## 2. Experimental Section

Experiments were conducted in the special transmission infrared cell adapted to combine FTIR and simultaneous UV excitation, as described in detail previously.[11,12] The cell is a stainless steel cube with six conflat flange ports. KBr windows, sealed with differentially pumped double O-rings, were used on two ports for infrared beam transmission. A UV-grade quartz window was used for ultraviolet irradiation. Samples were spray deposited on a tungsten support grid (0.0254 mm thick with 0.22 mm square openings exhibiting 70% optical transparency). The grid was secured by nickel clamps and mounted on electrical feedthroughs passing through the bottom of a reentrant Dewar which enters the cell. The grid and sample were heated electrically using a digital temperature programmer/controller.[13] Sample cooling was achieved by filling the reentrant Dewar with liquid nitrogen. A K-type thermocouple spot welded on the top center of the tungsten grid measured sample temperatures. The temperature could be held constant

(1) Wovchko, E. A.; Yates, J. T., Jr. *J. Am. Chem. Soc.* **1996**, *118*, 10250.
(2) Ballinger, T. H.; Yates, J. T., Jr. *J. Am. Chem. Soc.* **1992**, *114*, 10074.
(3) Ballinger, T. H.; Yates, J. T., Jr. *J. Phys. Chem.* **1992**, *96*, 9979.
(4) Wong, J. C. S.; Yates, J. T., Jr. *J. Am. Chem. Soc.* **1994**, *116*, 1610.
(5) Wong, J. C. S.; Yates, J. T., Jr. *J. Phys. Chem.* **1995**, *99*, 12640.
(6) Wovchko, E. A.; Yates, J. T., Jr. *J. Am. Chem. Soc.* **1995**, *117*, 12557.
(7) Wovchko, E. A.; Yates, J. T., Jr. *J. Am. Chem. Soc.* **1998**, *120*, 7544.
(8) Yang, A. C.; Garland, C. W. *J. Phys. Chem.* **1957**, *61*, 1504.
(9) Rice, C. A.; Worley, S. D.; Curtis, C. W.; Guin, J. A.; Tarrer, A. R. *J. Chem. Phys.* **1981**, *74*, 6487.
(10) Wey, J. P.; Neely, W. C.; Worley, S. D. *J. Catal.* **1992**, *134*, 378.
(11) Basu, P.; Ballinger, T. H.; Yates, J. T., Jr. *Rev. Sci. Instrum.* **1988**, *59*, 1321.
(12) Wong, J. C. S.; Linsebigler, A.; Lu, G.; Fan, J.; Yates, J. T., Jr. *J. Phys. Chem.* **1995**, *99*, 335.
(13) Muha, R. J.; Gates, S. M.; Yates, J. T., Jr.; Basu, P. *Rev. Sci. Instrum.* **1985**, *56*, 613.

S0002-7863(98)01241-4 CCC: $15.00 
Published on Web 09/24/1998

and maintained to ±2 K in the range 140−1500 K. The cell was connected via stainless steel bellows tubing to a bakeable stainless steel vacuum and gas delivery system. The system was pumped by 60 L $s^{-1}$ turbomolecular and 30 L $s^{-1}$ ion pumps achieving base pressures of $<1 \times 10^{-8}$ Torr. The system was equipped with a Dycor M100M quadrupole mass spectrometer for gas analysis and leak checking. Gas pressures were measured with a MKS 116A Baratron capacitance manometer.

The 0.5% $Rh/Al_2O_3$ samples were prepared by dissolving $RhCl_3 \cdot 3H_2O$ (Alfa 99.9%) in ultrapure $H_2O$ (10 mL/g of support). The solution was mixed with the appropriate amount of powdered $Al_2O_3$ (Degussa, 101 $m^2/g$) and ultrasonically dispersed for approximately 45 min. This slurry was then mixed with acetone (Mallinckrodt, AR) (9/1 acetone/$H_2O$ volume ratio) and sprayed onto the tungsten grid using a nitrogen-gas-pressured atomizer. The grid was warmed (∼330 K), and spraying was interrupted intermittently to allow for solvent evaporation. The mixture was sprayed on a two-thirds section (3.0 $cm^2$) of the grid, leaving a shielded one-third section (1.5 $cm^2$) clear for background scans. Deposit weights ranged from 23.3 to 27.6 mg (7.8 to 9.2 mg/$cm^2$) depending on the spraying time.

Immediately after spraying, the sample was transferred to the infrared cell and evacuated at 475 K for 16−20 h. Following evacuation the sample was reduced at 475 K using three 175-Torr $H_2$ exposures of 15 min each and one 200-Torr $H_2$ exposure of 60-min duration with evacuation after each exposure. The sample was evacuated at 475 K for another 18−20 h, then cooled to 303 K and exposed to 5 Torr of CO (or $^{13}C^{18}O$) for 10 min to convert the metallic Rh to $Rh^I(CO)_2$ [or $Rh^I(^{13}C^{18}O)_2$]. The cell was evacuated, and the sample was cooled to 141 K prior to $O_2$ addition. After $O_2$ addition, the sample was warmed to 174 K (181 K for the isotopically labeled rhodium *gem*-dicarbonyl experiment). The temperature never exceeded 176 K (183 K) during each experiment.

Infrared spectra were measured using a nitrogen-gas-purged Mattson Research Series I Fourier transform infrared spectrometer equipped with a liquid-nitrogen-cooled HgCdTe wide-band detector. Spectra were recorded by averaging 1000 scans at 4-$cm^{-1}$ spectral resolution and 250 scans at 4-$cm^{-1}$ resolution for the isotopically labeled rhodium *gem*-dicarbonyl experiment. The cell was translated laterally so the beam could pass through the unsprayed portion of the grid to obtain the background spectra. Small background features due to small deposits on the KBr windows were observed. Absorbance spectra of the sample were obtained by ratioing single-beam spectra of the sample to background single-beam spectra. Spectra have been offset slightly for better visualization.

A 350-W high-pressure mercury arc lamp provided the ultraviolet light for photolysis experiments. The optical bench was equipped with a *f*/1 two-element UV fused silica condensing lens, an iris diaphragm, and a shutter. The light was filtered by a 10-cm water infrared radiation filter and a 3.8 ± 0.5 eV (325 ± 50 nm) band-pass filter. Thermopile measurements indicate that the photon fluxes of the filtered UV light were $7.4 \times 10^{16}$ photons $cm^{-2}$ $s^{-1}$ ± 10% ($1.1 \times 10^{17}$ photons $cm^{-2}$ $s^{-1}$ ± 10% for isotope experiment). Photochemistry and infrared measurements were conducted simultaneously without disturbing the position of the cell or UV lamp. This was done by orienting the UV light source perpendicular to the infrared beam. The tungsten grid was aligned such that the infrared beam and the UV light were focused at a 45° angle to the normal of the grid.[12]

Carbon monoxide (Airco 99.999%) was obtained in an aluminum cylinder and transferred to a previously evacuated and baked glass bulb and used without further purification. Carbon dioxide (Matheson, 99.995%) and oxygen (Matheson, 99.998%) were obtained in steel cylinders and similarly transferred to previously evacuated and baked glass bulbs and used without further purification. Isotopically labeled $^{13}C^{18}O$ (Icon, 99% $^{13}C$, 95% $^{18}O$) was obtained in a glass breakseal flask and was used without further purification. Hydrogen (Matheson, 99.9995%) was obtained in a steel cylinder and was also used without further purification.

## 3. Results

**3.1. Photolysis of $Rh^I(CO)_2/Al_2O_3$ in $O_2$.** Infrared spectra measured during the photolysis of $Rh^I(CO)_2$ supported on $Al_2O_3$ in the presence of 7.9 Torr of $O_2$ at 174 K are shown in Figure 1. Two strong infrared bands are observed at 2100 and 2030 $cm^{-1}$ in the initial spectrum measured prior to any UV light exposure ($t_{UV} = 0$ min). These bands occur in the C−O region for the symmetric and antisymmetric stretching modes of $Rh^I(CO)_2$ (rhodium *gem*-dicarbonyl).[8,9,14−20] The isolated $Rh^I(CO)_2$ species are formed from the disruption of metallic Rh in a reaction with CO and hydroxyl groups (Al−OH) on the $Al_2O_3$ support.[14,15] The initial spectrum ($t_{UV} = 0$ min) was measured after 30 min of exposure to $O_2$ with no UV irradiation, and no loss of IR intensity was observed in the initial period.

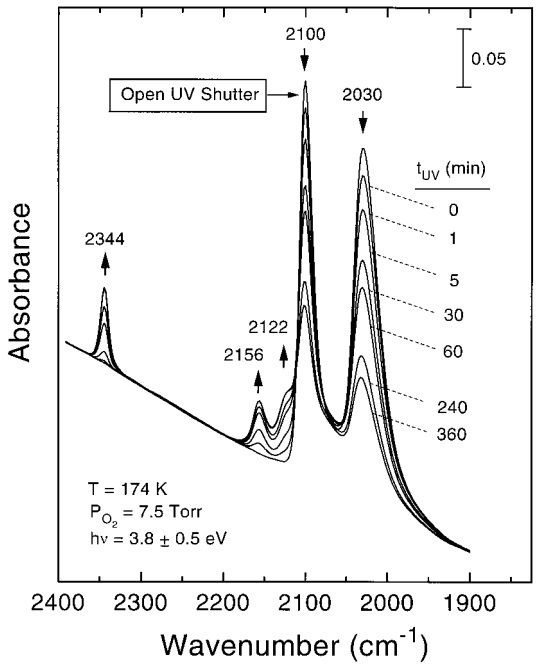


**Figure 1.** Infrared spectra measured in the C−O and $CO_2$ stretching regions during 360 min of photolysis of $Rh^I(CO)_2/Al_2O_3$ in the presence of 7.9 Torr of $O_2$ at 174 K. The arrows indicate the directions of the absorbance changes.

Immediately after opening the UV lamp shutter, the absorbance of the two bands at 2100 and 2030 $cm^{-1}$ decreases, indicating the depletion of $Rh^I(CO)_2$ species (the direction of absorbance change is shown by the arrows). Infrared spectra were continually measured at the indicated times ($t_{UV}$) following 1−360 min of ultraviolet photolysis. The depletion is accompanied by the formation of two overlapping infrared bands at 2156 and 2122 $cm^{-1}$. These two bands lie in the C−O stretching region and are due to the formation of new oxidized rhodium carbonyl species.[8−10] Another band develops at 2344 $cm^{-1}$, indicative of the formation of $CO_2$ species which are then adsorbed onto the $Al_2O_3$ support.[21−22] (Note that the CO and $CO_2$ designation corresponds to $^{12}C^{16}O$ and $^{12}C^{16}O_2$ in natural abundance. Also, $O_2$ corresponds to $^{16}O_2$ in natural abundance and was used in all experiments.) The formation of these bands

(14) Basu, P.; Panayotov, D.; Yates, J. T., Jr. *J. Phys. Chem.* **1987**, *91*, 3133.
(15) Basu, P.; Panayotov, D.; Yates, J. T., Jr. *J. Am. Chem. Soc.* **1988**, *110*, 2074.
(16) Yates, J. T., Jr.; Duncan, T. M.; Worley, S. D.; Vaughan, R. W. *J. Chem. Phys.* **1979**, *70*, 1219.
(17) Yates, J. T., Jr.; Duncan, T. M.; Vaughan, R. W. *J. Chem. Phys.* **1979**, *71*, 3908.
(18) Cavanagh, R. R.; Yates, J. T., Jr. *J. Chem. Phys.* **1981**, *74*, 4150.
(19) Yates, J. T., Jr.; Kolasinski, K. *J. Chem. Phys.* **1983**, *79*, 1026.
(20) Solymosi, F.; Pásztor, M. *J. Phys. Chem.* **1985**, *89*, 4789.
(21) Parkyns, N. D. *J. Phys. Chem.* **1971**, *75*, 526.
(22) Peri, J. B. *J. Phys. Chem.* **1966**, *70*, 3168.

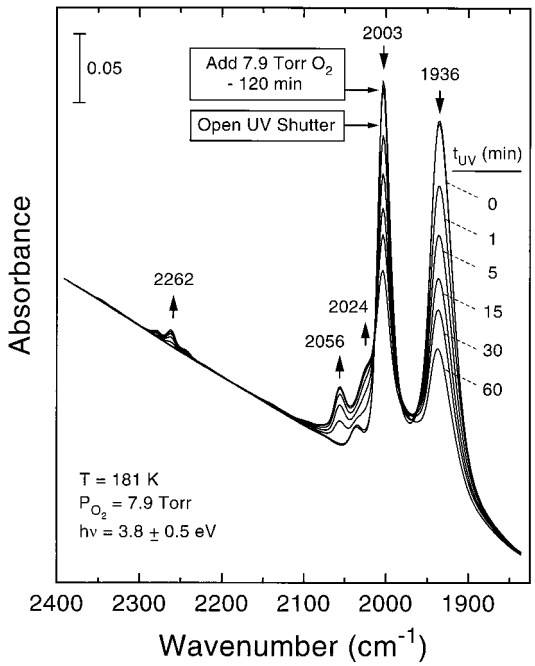


**Figure 2.** Infrared spectra measured in the C−O and $CO_2$ stretching regions during 60 min of photolysis of $Rh^I(^{13}C^{18}O)_2/Al_2O_3$ in the presence of 7.9 Torr of $O_2$ at 181 K. The arrows indicate the directions of the absorbance changes.

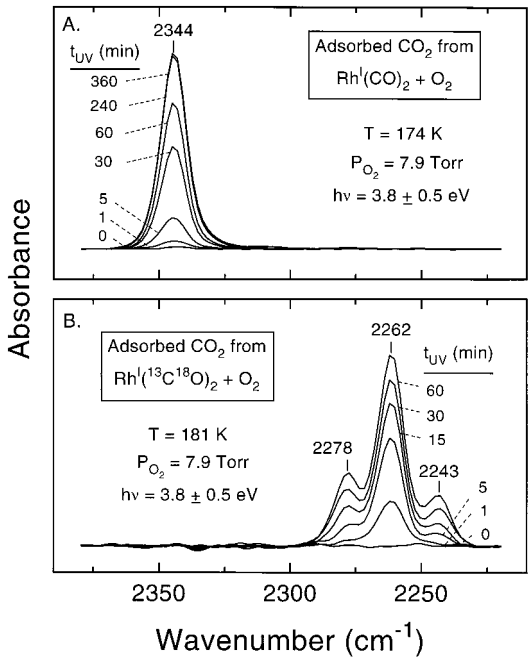


**Figure 3.** Analysis of the adsorbed carbon dioxide antisymmetric stretching modes during the photoassisted CO oxidation in both unlabeled and labeled isotopic experiments. Part A shows the expanded $CO_2$ spectrum during $O_2$ activation on $Rh^I(CO)_2/Al_2O_3$. Part B shows the expanded carbon dioxide region during $O_2$ activation on $Rh^I(^{13}C^{18}O)_2/Al_2O_3$. (Note: spectra have been baseline corrected.)

indicates the activation of the O═O bond in $O_2$ and subsequent CO ligand oxidation as a result of UV irradiation at 174 K.

To verify the activation of $O_2$ and the CO oxidation, a similar experiment was conducted using isotopically labeled $Rh^I(^{13}C^{18}O)_2$. The infrared spectra measured following 1−60 min of photolysis (at a slightly higher photon flux) of $Rh^I(^{13}C^{18}O)_2$ in the presence of 7.9 Torr of $O_2$ at 181 K is presented in Figure 2. The initial spectrum, measured prior to $O_2$ exposure, displays appropriately shifted infrared bands at 2003 and 1936 $cm^{-1}$ for the symmetric and antisymmetric stretching modes of isotopically labeled $Rh^I(^{13}C^{18}O)_2$.[1,7] A small band is observed at 2036 $cm^{-1}$ for $Rh^I(^{13}C^{16}O)(^{13}C^{18}O)$ species due to the 5% $^{13}C^{16}O$ impurity in the isotopically labeled $^{13}C^{18}O$. The cell was then filled with 7.9 Torr of $O_2$ and allowed to sit at 181 K for 120 min prior to recording a second spectrum before UV light exposure ($t_{UV}$ = 0 min). Only a very small loss in the original intensity of the *gem*-dicarbonyl species is observed.

The UV lamp shutter was opened, allowing the sample to be irradiated. The absorbance of the two bands at 2003 and 1936 $cm^{-1}$ continually decreases as photolysis progresses. The depletion of $Rh^I(^{13}C^{18}O)_2$ species is accompanied by the development of two overlapping infrared bands centered at 2056 and 2024 $cm^{-1}$. These bands occur at lower frequency and are very similar in nature to the 2156- and 2122-$cm^{-1}$ bands observed during the unlabeled $Rh^I(CO)_2$ photoassisted oxidation (Figure 1). These bands are assigned to oxidized rhodium carbonyl species containing different CO isotopomers ($^{12}C^{16}O$; $^{13}C^{18}O$). A set of overlapping infrared features centered at 2262 $cm^{-1}$ is observed due to the formation of isotopically labeled carbon dioxide species adsorbed on the $Al_2O_3$ support.[23] The production of isotopically labeled oxidized rhodium carbonyl features and isotopically labeled carbon dioxide features in the spectra achieved during photolysis indicates that CO oxidation involves the CO ligand of the photochemically produced $Rh^I(CO)$ species.

**3.2. Analysis of the Carbon Dioxide Infrared Features.** The infrared features caused by carbon dioxide formation in the above experiments (Figures 1 and 2) are shown in more detail in Figure 3. The set of spectra measured during the photolysis of $Rh^I(CO)_2$ in $O_2$ is shown in Figure 3A. The single feature centered at 2344 $cm^{-1}$ for carbon dioxide adsorbed on the $Al_2O_3$ support becomes more intense with increased photolysis time. The infrared spectra measured during photolysis of isotopically labeled $Rh^I(^{13}C^{18}O)_2$ in the presence of $O_2$ are displayed in Figure 3B. No absorption features are observed near 2344 $cm^{-1}$, which is characteristic of unlabeled carbon dioxide. Instead, three overlapping bands at 2278, 2262, and 2243 $cm^{-1}$ develop with increased UV irradiation. These three features represent three species of isotopically labeled carbon dioxide adsorbed on the $Al_2O_3$ support, $^{16}O^{13}C^{16}O$, $^{16}O^{13}C^{18}O$, and $^{18}O^{13}C^{18}O$.[23−26] The most intense feature is the 2262-$cm^{-1}$ feature followed by the much weaker 2278-$cm^{-1}$ feature and then the 2243-$cm^{-1}$ feature. These intensity differences reflect the relative amounts of the carbon dioxide isotopomers produced by photochemical oxidation of $^{13}C^{18}O$ ligands.

Infrared band frequencies for each of the adsorbed carbon dioxide isotopomers are presented in Table 1 along with gas-phase frequencies and frequencies predicted for a linear triatomic oscillator using the appropriate masses and a force constant of $14.13 \times 10^5$ dyn $cm^{-1}$. The force constant was calculated from the frequency of the observed antisymmetric stretching mode of unlabeled adsorbed $CO_2$.[27]

## 4. Discussion

**4.1. Photochemistry of $Rh^I(CO)_2/Al_2O_3$ in $O_2$: Formation of Oxidized Rhodium Carbonyl Species.** The ultraviolet

(23) Herzberg, G. *Molecular Spectra and Molecular Structure II*, 7th ed.; D. Van Nostrand Co.: Princeton, NJ, 1956; p 274.

(24) Nielsen, A. H. *Phys. Rev.* **1938**, *53*, 983.

(25) Fredin, L.; Nelander, B.; Ribbegård, G. *J. Mol. Spectrosc.* **1974**, *53*, 410.

(26) Berney, C. V.; Eggers, D. F., Jr. *J. Chem. Phys.* **1964**, *40*, 990.

(27) Herzberg, G. *Molecular Spectra and Molecular Structure II*, 7th ed.; D. Van Nostrand Co.: Princeton, NJ, 1956; pp 172−174.

**Table 1.** Spectroscopic Assignments of the Asymmetric Stretching Modes of Adsorbed Carbon Dioxide Isotopomers on $Al_2O_3$ Using Gas-Phase Frequencies and Frequencies Calculated Using a Linear Triatomic Oscillator Model and a Force Constant[a] of $14.13 \times 10^5$ dyn cm$^{-1}$ [27]

| species | $\nu_{asym}$(obsd), cm$^{-1}$ | $\nu_{asym}$(calcd), cm$^{-1}$ | $\nu_{asym}$(gas phase), cm$^{-1}$ | ref |
|---|---|---|---|---|
| $^{12}C^{16}O_2$ | 2344 | | 2349 | 23 |
| $^{13}C^{16}O_2$ | 2278 | 2278 | 2283 | 24 |
| $^{13}C^{16}O^{18}O$ | 2262 | 2260 | 2266 | 26 |
| $^{13}C^{18}O_2$ | 2243 | 2241 | 2247 | 26 |

[a] The force constant of $14.13 \times 10^5$ dyn cm$^{-1}$ was determined from the asymmetric stretching frequency for adsorbed $^{12}C^{16}O_2$ (2344 cm$^{-1}$) observed in this work.

photolysis of $Rh^I(CO)_2/Al_2O_3$ results in the loss of a CO ligand and the production of coordinatively unsaturated $Rh^I(CO)$. Here we have utilized these photochemically generated $Rh^I(CO)$ catalyst sites to activate the O═O bond in $O_2$ and to cause the oxidation of CO to occur at low temperature (174 K).

As photolysis proceeds, rhodium *gem*-dicarbonyl species are depleted. New infrared bands are observed in the C−O stretching region at higher frequencies than those of the original $Rh^I(CO)_2$ infrared bands (Figure 1). These bands arise from the oxidative addition of $O_2$ to the unstable, coordinatively unsaturated $Rh^I(CO)$ to form oxidized rhodium carbonyl species as shown below. The higher frequency mode at 2156 cm$^{-1}$ is assigned to $Rh^{IV}(CO)(O)_2$, and the mode at 2122 cm$^{-1}$ is assigned to $Rh^{II}(CO)(O)$ species.

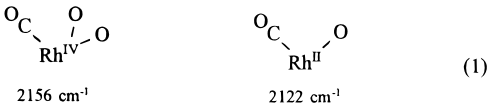


(1)

The transition state during the oxidative addition of $O_2$ is expected to involve a three-membered ring species prior to $O_2$ dissociation.

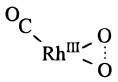


(2)

Unfortunately, we were unable to examine the infrared spectrum near 875−900 cm$^{-1}$ for the expected stretching vibration of dioxygen coordinated to the Rh center.[28−30] This is due to the strongly absorbing vibrational modes of the aluminum oxide support which essentially cut off infrared transmission below 1000 cm$^{-1}$. Therefore, we are unable to distinguish $Rh^{IV}(CO)(O)_2$ from $Rh^{III}(CO)(O_2)$ on the basis of O−O vibrational modes.

The formal oxidation state of Rh changes from $Rh^I$ to $Rh^{IV}$ as $O_2$ dissociatively coordinates to $Rh^I(CO)$ species. The shift to higher frequency of the infrared band for the remaining CO ligand occurs as a result of the increase in the oxidation state of Rh. The following rhodium monocarbonyl species have been characterized by Rice et al.[9] on $Rh/Al_2O_3$ catalysts: $Rh^{III}(CO)$, $\nu_{CO} = 2136$ cm$^{-1}$; $Rh^{II}(CO)$, $\nu_{CO} = 2125$ cm$^{-1}$; $Rh^I(CO)$, $\nu_{CO} \approx 2100$ cm$^{-1}$. Less back-donation into the $2\pi^*$ antibonding orbital is experienced by the CO ligand bound to Rh at higher oxidation states, resulting in an increase of the CO stretching frequency as the Rh oxidation state increases.[31,32]

**Table 2.** Spectroscopic Assignment of Various Rhodium Carbonyl Species

| Species | $\nu_{CO}$ cm$^{-1}$ | Ref. |
|---|---|---|
| 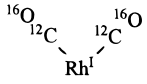 | 2100 ; 2030 | [1-6,14-20] |
| 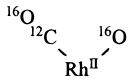 | 2122 | This work, [8,10] |
| 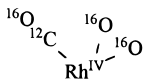 | 2156 | This work |
| 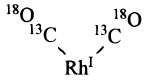 | 2003 ; 1936 | This work, [1,7] |
| 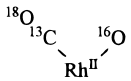 | 2024 | This work |
| 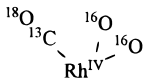 | 2056 | This work |
| $Rh^{III}Cl_3(^{12}C^{16}O) \cdot 2\ H_2O$ | 2136 | [9] |

The $Rh^{II}(CO)(O)$ species has been characterized previously.[8−10] and the stretching frequency for the CO ligand occurs in the range 2125−2116 cm$^{-1}$. Our measured frequency of 2122 cm$^{-1}$ falls into this range. The 2136-cm$^{-1}$ feature observed in the work of Rice et al.[9] was assigned to a $Rh^{III}(CO)$ species produced in a reaction of CO with unreduced $Rh^{III}Cl_3 \cdot 3H_2O/Al_2O_3$. We assign the newly identified 2156-cm$^{-1}$ feature observed in this work to $Rh^{IV}(CO)(O)_2$ species. The assignments of the observed species are summarized in Table 2.

**4.2. Mechanism for CO Oxidation on $Rh^I(CO)$ Sites.** The dissociation of $O_2$ on $Rh^I(CO)$ sites results in the oxidation of the CO ligand to form carbon dioxide species. The oxidation of CO is also readily observed on metallic and supported Rh catalysts at elevated temperatures (>500 K).[33−35] In the work presented here, the oxidation of CO takes place at cryogenic temperatures (∼174 K) on isolated $Rh^I(CO)$ sites produced photochemically. No substantial $CO_2$ formation was observed by thermally excited processes at 174−181 K (Figures 1 and 2).

A simple mechanism for $O_2$ activation on $Rh^I(CO)_2/Al_2O_3$ and CO oxidation is proposed in Figure 4. The photolysis of $Rh^I(CO)_2$ species results in the reversible loss of a carbon

(28) Mieczynska, E.; Trzeciak, A. M.; Ziólkowski, J. J.; Tadeusz, L. *J. Am. Chem. Soc., Dalton Trans*. **1995**, 105.
(29) Haarman, H. F.; Bregman, F. R.; van Leeuwen, P. W. N. M.; Vrieze, K. *Organometallics* **1997**, *16*, 979.
(30) Selke, M.; Karney, W. L.; Khan, S. I.; Foote, C. S. *Inorg. Chem.* **1995**, *34*, 5715.
(31) Huheey, J. E. *Inorganic Chemistry: Principles of Structure and Reactivity*, 3rd ed.; Harper & Row: New York, 1983; Chapter 9.
(32) Butler, I. S.; Harrod, J. F. *Inorganic Chemistry: Principles and Applications*; Benjamin/Cummings: Redwood City, CA, 1989; Chapter 22.
(33) Peden, C. H. F.; Goodman, D. W.; Blair, D. S.; Berlowitz, P. J.; Fisher, G. B.; Oh, S. H. *J. Phys. Chem.* **1988**, *92*, 1563.
(34) Goodman, D. W.; Peden, C. H. F. *J. Phys. Chem.* **1986**, *90*, 4839.
(35) Oh, S. H.; Fisher, G. B.; Carpenter, J. E.; Goodman, D. W.*J. Catal.* **1986**, *100*, 360.

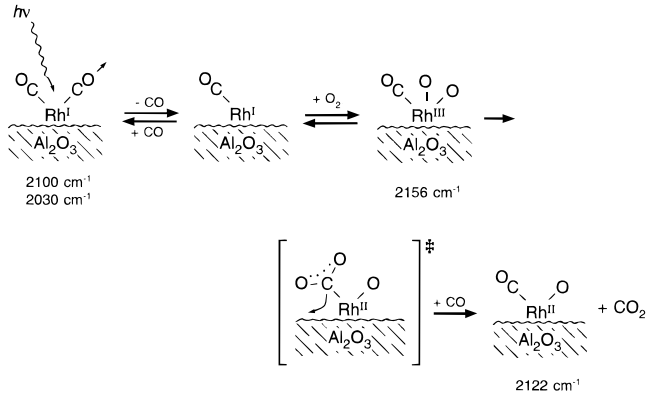


**Figure 4.** Proposed mechanism for the activation of $O_2$ on photochemically generated $Rh^I(CO)$ sites.

monoxide ligand to form the coordinatively unsaturated $Rh^I(CO)$ site. The site may either absorb a CO molecule from the gas phase to regenerate the gem-dicarbonyl species or coordinate with $O_2$ in an oxidative addition reaction to form $Rh^{IV}(CO)(O)_2$ species which is detected spectroscopically by means of a high-frequency C−O stretching mode. Upon addition of CO from the gas phase, dissociation of the O═O bond occurs, leading to the formation of a $CO_2$ ligand coordinated to the Rh center. Carbon dioxide is eliminated, forming $Rh^{II}(CO)O$ species. The $CO_2$ is then bound to the $Al_2O_3$ support, through surface migration and/or adsorption from the gas phase.

One may realize that the above description is a simplified representation of a more complicated overall oxidation process. This is evident from the results of the photolysis experiment of isotopically labeled $Rh^I(^{13}C^{18}O)_2$ in $O_2$ (Figures 2 and 3). According to the proposed reaction scheme in Figure 4, the major oxidation product is $^{13}C^{16}O^{18}O$. Although $^{13}C^{16}O^{18}O$ was produced in highest concentration, as judged by the relative absorbances in Figure 3, all three possible isotopomers of carbon dioxide were generated. The production of $^{13}C^{16}O_2$, $^{13}C^{16}O^{18}O$, and $^{13}C^{18}O_2$ indicates that a more complex isotopic mixing process takes place in the final stage of the reaction between the $^{13}C^{18}O$ and $^{16}O$ ligands of $Rh^{IV}(^{13}C^{18}O)(^{16}O)_2$ during the transformation of $Rh^{IV}(CO)(O)_2$ species to $Rh^{II}(CO)(O) + CO_2$. We observed a similar isotopic mixing process taking place during the photochemical activation of $CO_2$ on $Rh^I(CO)$ sites.[7] It is likely in the present experiments that, during the photochemical production of $^{13}C^{16}O^{18}O$, this species is itself activated upon readsorption on $Rh^I(CO)$ sites, producing the other two isotopomers of $CO_2$ through interaction with either $^{13}C^{18}O$ ligands or $^{13}C^{16}O$ ligands on the $Rh^I$ center.

## 5. Conclusions

The following conclusions have been reached concerning the activation of $O_2$ on coordinatively unsaturated $Rh^I(CO)$ sites produced photochemically from $Rh^I(CO)_2$:

(1) Dioxygen is activated on photochemically generated $Rh^I(CO)$ sites to produce highly oxidized rhodium carbonyl species. A new infrared band at 2156 $cm^{-1}$ is assigned to the formation of the $Rh^{IV}(CO)(O)_2$ species. A band at 2122 $cm^{-1}$ is assigned to the formation of the $Rh^{II}(CO)(O)$ species.

(2) Photoassisted CO oxidation takes place at cryogenic temperatures (174 K) to form carbon dioxide, which then becomes bound to the $Al_2O_3$ support, through surface migration and/or adsorption from the gas phase.

(3) The photolysis of isotopically labeled $Rh^I(^{13}C^{18}O)_2$ in $O_2$ results in the production of $^{13}C^{16}O_2$, $^{13}C^{16}O^{18}O$, and $^{13}C^{18}O_2$. The production of three isotopomers of carbon dioxide during CO oxidation indicates that the $CO_2$ product may itself become activated by readsorption on $Rh^I(CO)$ sites produced under photochemical conditions, as has been seen in previous work.[7]

**Acknowledgment.** We thank the Department of Energy, Office of Basic Energy Sciences, for support of this work.

JA981241Y